

We are IntechOpen, the world's leading publisher of Open Access books Built by scientists, for scientists

4,800

Open access books available

122,000

International authors and editors

135M

Downloads

Our authors are among the

154

Countries delivered to

TOP 1%

most cited scientists

12.2%

Contributors from top 500 universities



WEB OF SCIENCE™

Selection of our books indexed in the Book Citation Index
in Web of Science™ Core Collection (BKCI)

Interested in publishing with us?
Contact book.department@intechopen.com

Numbers displayed above are based on latest data collected.

For more information visit www.intechopen.com



Damage Assessment of Short Glass Fiber Reinforced Polyester Composites: A Comparative Study

Amar Patnaik¹, Sandhyarani Biswas²,
Ritesh Kaundal¹ and Alok Satapathy²

¹*Department of Mechanical Engineering, National
Institute of Technology, Hamirpur*

²*Department of Mechanical Engineering, National
Institute of Technology, Rourkela
India*

1. Introduction

The main goals of many challenges to the utilization of by-product cement kiln dusts (CKDs) as partial replacement of Portland cement (PC) environmental protection agencies are to seek ways to minimize the dual problems of disposal and health hazards of these by-products. For many years, by-products such as fly-ash, silica fume and slag were considered as waste materials. These by-products have been successfully used in the construction industry as a portland cement substitute (Krazowski & Emery, 1981; Al-jabri et al., 2006). However, with the growing of industries the new and different types of by-products are being generated by various industries, which could have being a promising future for partial replacement of portland cement. CKDs typically fine powders that are generated during the cement manufacturing process, and then carried off in the flue gases then subsequently collected in electrostatic precipitators. The portion of CKDs that are not returned back to the cement manufacture process, or otherwise used beneficially, are placed in landfills. A limited number of studies have carried out the use of CKD as industrial wastes in fabrication of polymer composites. The effect of CKD on the compressive strength of cement paste was studied and the corrosion behavior of embedded reinforcement and observed that up to 5wt% of CKD of cement had less effect on cement paste strength and on reinforcement (El-Sayed et al., 1991). It has also reported that when CKD and blast furnace slag are added in proper ratio to ordinary cement, the compressive strength and the corrosion-resistance of the mix increase dramatically (Batis et al., 2002). It has also been reported that the use of CKD in concrete as a partial replacement of cement (Sri Ravindrarajah, 1982). The percentages of cement replacement by weight were in different percentage i.e. from 0, 25, 50, 75, and 100 in cement paste and 0, 15, 25, 35, and 45 in both 1:1.5:3 and 1:2:4 concretes. As CKD is a cementitious material and it showed good strength as compared with general cement. Therefore, particulate played a vital role in the development of commercially feasible fiber reinforced polymers. Not only they provide significant cost reductions but also certain fillers may improve processing, physical properties and improved the mechanical strength (Rothon, 2002). There are few, if any,

publications exploring the effect of hard ceramic particles on the wear resistance (especially for erosion resistance) of composites. Further, there are few publications discussing the erosion wear mechanisms of elastomers and their composites. Based on the above study, computational simulation has provided an effective and economical approach to study wear problems. During past decades, there were a number of computational models proposed to simulate wear processes at macro/meso and atomic/nano-scales (Ling & Pan, 1986; Ludema & Bayer, 1991; Hsu et al., 1997; Komvopoulos & Choi, 1992). The most widely used macro/meso-scope model is FEM (finite element method), which can be used to deal with elastic/plastic contact problems and failure processes in the contact region. The two-dimensional (2D) water drop impact model with DYNA3D code was established (Adler, 1995). The calculation did not involve any solid erodent. Despite this, to date there are no economically viable and environmentally acceptable solutions for effective utilization of the high-residue volumes that have developed. Current best practice is to contain the material within specially constructed landfill sites, called red mud ponds/stacks or bauxite residue disposal areas (BRDAs). Recently, the potential utilization of red mud filled glass/bamboo epoxy composites was explored and investigated its significant effect on the erosion wear rate of the resulting composites (Biswas and Satapathy, 2009, 2010). Few researchers also studied the solid particle erosion behavior of particulate filled polymer matrix composites and revealed that parameters such as impact velocity, impingement angle, fiber loading/filler content, erodent size, erodent temperature and stand-off distance etc. largely depends on the erosion behavior of polymer composites (Patnaik et al., 2010a, 2010b, 2010c, 2010d, 2010e, 2010f, 2010g).

In view of the above literature in this work, a non-linear finite element model has been proposed and compared the simulated results with experimental results. The utility of the new formulation is proven through its application onto a short glass fiber reinforced polyester based composites filled with cement by-pass dust as reinforcing particulates. This model is simple and flexible, which helps to gain insight into various wear processes. The eroded surfaces of these composites are analyzed with scanning electron microscopy (SEM), and the erosion wear mechanisms of the composites are investigated.

2. Experimental

2.1 Preparation of composites

Short glass fibers (elastic modulus of 72.5 GPa and possess a density of 2.59 gm/cc) of 6mm length are used to prepare the composites. The unsaturated isophthalic polyester resin (Elastic modulus 3.25GPa, density 1.35gm/cc) is manufactured by Ciba Geigy and locally supplied by Northern Polymers Ltd. New Delhi, India. The composite fabricated in two different sets. One having different fiber loading, with varying the weight fraction of fibers from 10wt% to 50wt% at an increment of 10wt% and the designation of individual composites are reported in Table 1. Secondly, cement by-pass dust (CBPD) particulate is mixed with short glass fiber reinforced polyester resin with three different percentages (0wt%, 10wt% and 20wt% of CBPD) and the mixture is poured into various moulds conforming to the requirements of various testing conditions and characterization standards. The entrapped air bubbles (if any) are removed carefully with a sliding roller and the mould is closed for curing at a temperature of 30°C for 24 h at a constant pressure of 10 kg/cm².

2.2 Air-jet erosion tester

The erosion experiments are carried out as per ASTM G76 on the erosive wear test rig. The equipment was designed to feed abrasive particles into a high velocity air stream, which

| Sl. No. | Designation of composites | Composition of composites |
|---------|---------------------------|---|
| 1. | PGFL-1 | Polyester resin + 10wt% Short glass fiber |
| 2. | PGFL-2 | Polyester resin + 20wt% Short glass fiber |
| 3. | PGFL-3 | Polyester resin + 30wt% Short glass fiber |
| 4. | PGFL-4 | Polyester resin + 40wt% Short glass fiber |
| 5. | PGFL-5 | Polyester resin + 50wt% Short glass fiber |

Table 1. Designation and composition of unfilled short glass fiber reinforced composites

propelled the particles against the specimen surface (Strzepa et al., 1993; Routbort et al., 1981). The erodent particles entrained in a stream of compressed air and accelerated down to a 65mm long brass nozzle with 3mm inside diameter to impact on a target material mounted on an angle fixture. The steady state erosion rates are measured as a function of the erodent particle size and the amount of erodent particle used in each experiment was measured with the help of double disc method. The steady state erosion rate was determined by weighing the sample after the end of each test. While the impingement angles ranges from 30° to 90° and the test duration was 20min for each run. The erodent used for this test was river silica sand particle of three different sizes, i.e. 250, 350 and 450µm. The sample was cleaned with a blast of compressed air before each weighing to remove all loosely adhering debris. The mass loss from the target was measured with an analytical balance of ±0.01mg accuracy. The erosion rate was measured in terms of mass of material removed per unit mass of erodent impacted. The process is repeated every 10 min till the erosion rate attains a constant value called steady-state-erosion-rate.

2.3 Finite element model

The erosive processes are simulated using an explicit dynamic code ANSYS/AUTO-DYN. The eight-node brick hexahedral elements with one integration point are used in the 3D simulation. The mesh is refined to standard cubic element at the impacted area in order to calculate the erosion rate. It has reported in literature that simulating a single particle was not sufficient and three or more particles were needed to simulate the erosion process (EITobgy et al., 2005). In this study, 100 spherical particles were used so as to ensure the accuracy of the model. All of the particles strike the target center area at random locations. The “simultaneous group” was employed for computational efficiency and analytical organization. There are 10 groups which contain 100 particles aggregately in the proposed model. Every group has 10 particles which would impact the surface simultaneously and be followed by another simultaneous particles group, and so on. According to the researchers, the distance between any two particles’ centers in the same group is no less than 0.6r (r is the radius of the particles) to avoid the damage interaction (Woytowitz and Richman, 1999). Figure 1 shows the schematic diagram of the prepared composites by using ANSYS/AUTO-DYN. The finite element model of the target material and simulated nozzle is shown in Figure 2. There are 164, 765 nodes and 147, 840 finite elements in the model. All of the bottom nodes of the target materials are fixed. For the particles, the rotation degrees of freedom are constrained. Generally, the erosion rate (gm/gm) was used to characterize the erosion performance of the target materials. The solution time is set to 1.3t10, where t10 is the time when the last particles group contacted to the target. In this study, the impact angle varies from 30° to 90° in increments of 15°. The impact velocity varies from 43 to 65 m/s.

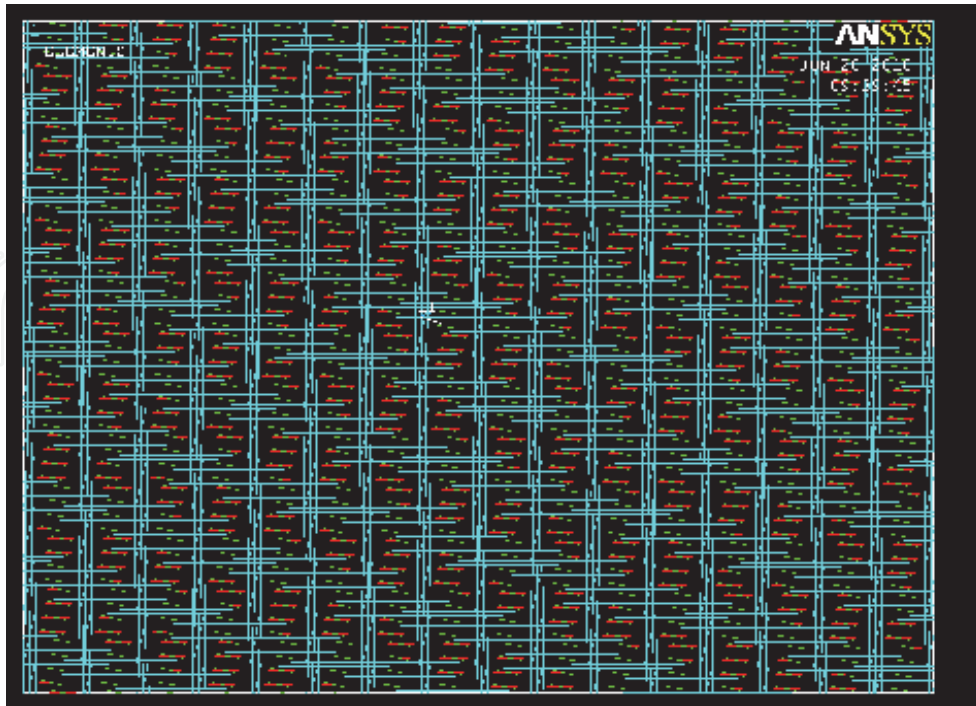


Fig. 1. Schematic diagram of the particulate filled composite

2.4 Plan of experiments (Taguchi's techniques)

For the elaboration of experiments plan, the method of Taguchi for five control factors at three levels is used, being understood by levels taken by the factors. Table 2 represents the factors to be studied and the assignment of the corresponding levels. The array chosen is the L_{27} (3^{13}) which has 27 rows corresponding to the number of tests (22 degrees of freedom) with 13 columns at three levels. The factors and the interactions are assigned to the columns. In practice, these factors can be assigned arbitrarily to any of the arrays columns, provided that all combinations must be included as per orthogonal array design. After assigning appropriate level settings, the S/N analysis (S/N: signal-to-noise ratio) is needed to evaluate the proposed experiment results. In S/N analysis, the greater the S/N, the better the experimental results:

$$\eta = -10 \log (\text{M.S.D.}) \quad (1)$$

where M.S.D. is the mean-square deviation for the output characteristic (erosive wear rate). As mentioned earlier, there are three categories of quality characteristics, i.e. lower-the-better, higher-the-better, and nominal-the-better. To obtain optimal performance, lower-the-better characteristic for erosion rate must be taken. The mean-square deviation (M.S.D.) for the lower-the-better characteristic can be expressed as (Glen, 1993):

$$\text{M.S.D} = \frac{1}{m} \sum_{i=1}^m T_i^2 \quad (2)$$

where m is the number of tests and T_i is the value of experimental result of the i^{th} test.

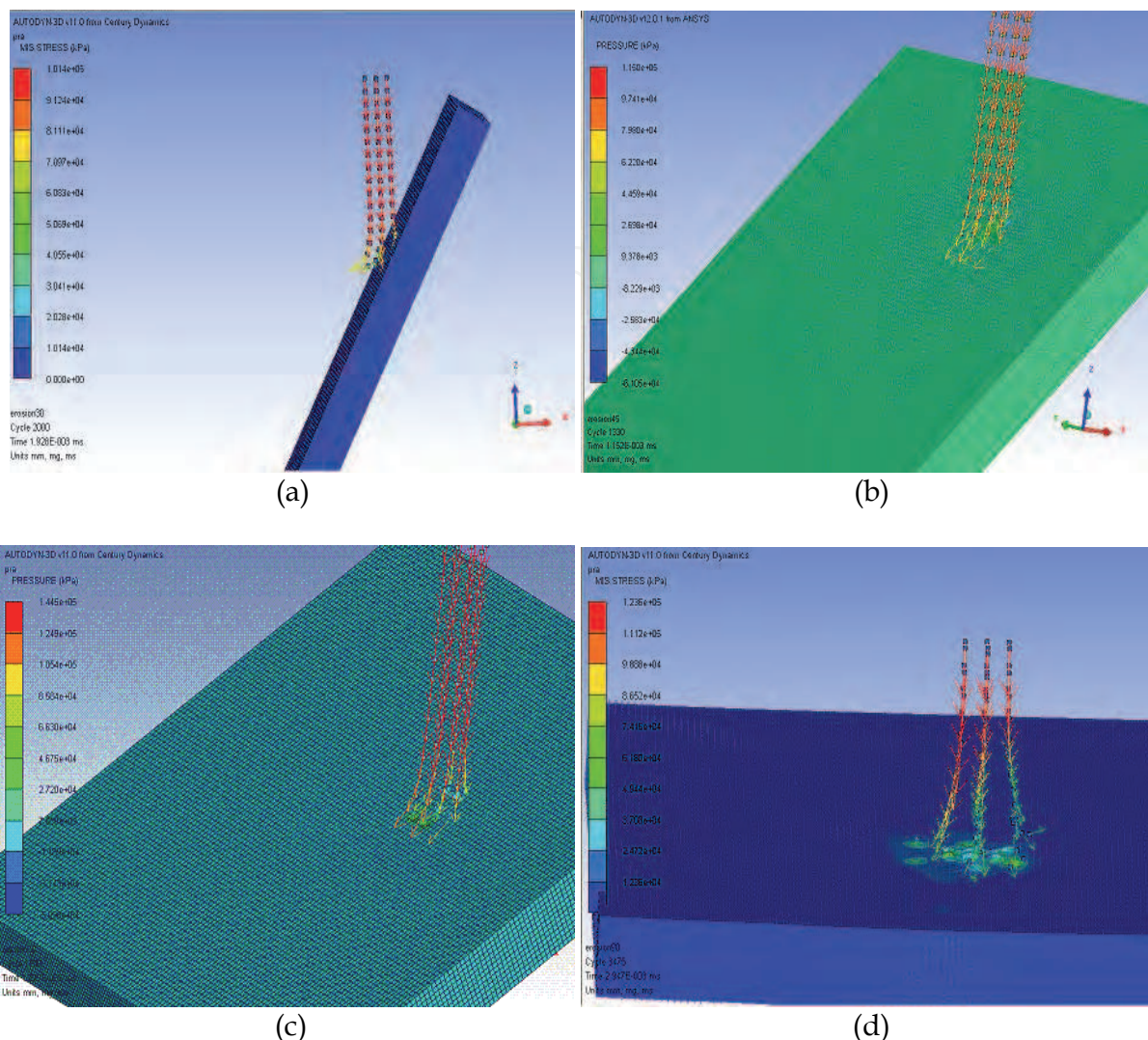


Fig. 2. Schematic diagram of target composite material and nozzle (a: 30° impingement angle, b: 45° impingement angle, c: 60° impingement angle and d: 90° impingement angle)

The plan of the experiments is as follows: the first column is assigned to impact velocity (A), the second column to CBPD content (B), the fifth column to impingement angle (C), the ninth column to stand-off distance (D) and the tenth column to erodent size (E), the third and fourth column are assigned to $(A \times B)_1$ and $(A \times B)_2$ respectively to estimate interaction between impact velocity (A) and CBPD percentage (B), the sixth and seventh column are assigned to $(B \times C)_1$ and $(B \times C)_2$ respectively to estimate interaction between the CBPD content (B) and impingement angle (C), the eighth and eleventh column are assigned to $(A \times C)_1$ and $(A \times C)_2$ respectively to estimate interaction between the impact velocity (A) and impingement angle (C) and the remaining columns are used to estimate experimental errors. The output to be studied is erosion rate (E_r) and the tests are repeated twice corresponding to 54 tests. Furthermore, a statistical analysis of variance (ANOVA) is performed to identify the process parameters that are statistically significant. With the S/N and ANOVA analyses, the optimal combination of the process parameters can be predicted to a useful level of accuracy. Finally, a confirmation experiment is conducted to verify the optimal process parameters obtained from the parameter design.

| Control factor | Level | | | Units |
|----------------------|-------|-----|-----|---------------|
| | I | II | III | |
| A:Velocity of impact | 43 | 54 | 65 | m/sec |
| B:CBPD content | 0 | 10 | 20 | % |
| C:Impingement angle | 30 | 60 | 90 | degree |
| D:Stand-off distance | 65 | 75 | 85 | mm |
| E:Erodent size | 250 | 350 | 450 | μm |

Table 2. Levels for various control factors

3. Results and discussion

3.1 Erosive wear of the composites

The erosive wear output characteristics are systematically determined by the Taguchi's technique as a multi-parametric optimization model, since the erosive wear may be a functional variable of five independent control factors and their interactions. Using this technique (a) firstly the steady state erosion characteristics of the composites are determined for selected level of optimally controlled operating variables and (b) subsequently control factors have been identified by Taguchi experimental techniques.

3.1.1 Effect of impingement angle on erosion rate

Solid-particle erosion is a complex wear mechanism, influenced by a number of factors such as impact velocity, impingement angle, erodent size, erodent temperature, stand-off distance, materials properties, particles geometry, environment temperature etc. Among these, angle of impingement is the one of the most important factor and widely studied parameter in the erosion study of materials (Hutchings, 1992; Tsuda et al., 2006). When the erosion rate is measured as a function of impingement angle, two types of material behavior generally observed in the target material i.e. ductile and brittle nature. The ductile behavior of materials is characterized by maximum erosion at acute angle (15-30°) and for brittle behavior of materials, the maximum erosion is observed at normal impingement angle (90°). But as far as polymer composites are concerned the composite materials show versatile in nature depending upon the fabrication techniques and the erosion rate show slightly different behavior. The reinforced composites show a semi-ductile behavior having the maximum erosion rate in the range of 45-60° (Hutchings, 1992), unlike the above two categories. This classification, however, is not absolute as the erosion of material has a strong dependence on erosion conditions such as the properties of target material. In the present study, Figure 3 shows that maximum erosion rate appears at 60°, indicating semi-ductile erosion behavior irrespective of fiber loading.

3.1.2 Surface morphology

Generally surface morphology of eroded surfaces indicates whether solid particle erosive wear has been occurred either by a ductile or brittle mechanism. Hence, scanning electron microscopy (SEM) studies have been done to ascertain the wear mechanism at 30°, 60° and 90° impingement angles. Figure 4a show micrographs of eroded surfaces of 10wt% short glass fiber reinforced polyester composites at 30° and 90° impingement angles at constant impact velocity of 43m/s, stand-off distance 75mm and erodent size 450 μm . It is evident from the micrograph (Figure 4a) that the material removal in the composite is dominated by

micro-ploughing, micro-cutting and plastic deformation. The plastically deformed material subsequently removed from the surface by micro-cutting leads to maximum erosion rate at 60° impingement angle; most material is lost when a maximum strain in the target is exceeded and formation of micro-cracks and embedment of fragments of sand particles is evident from the micrograph (Figure 4b).

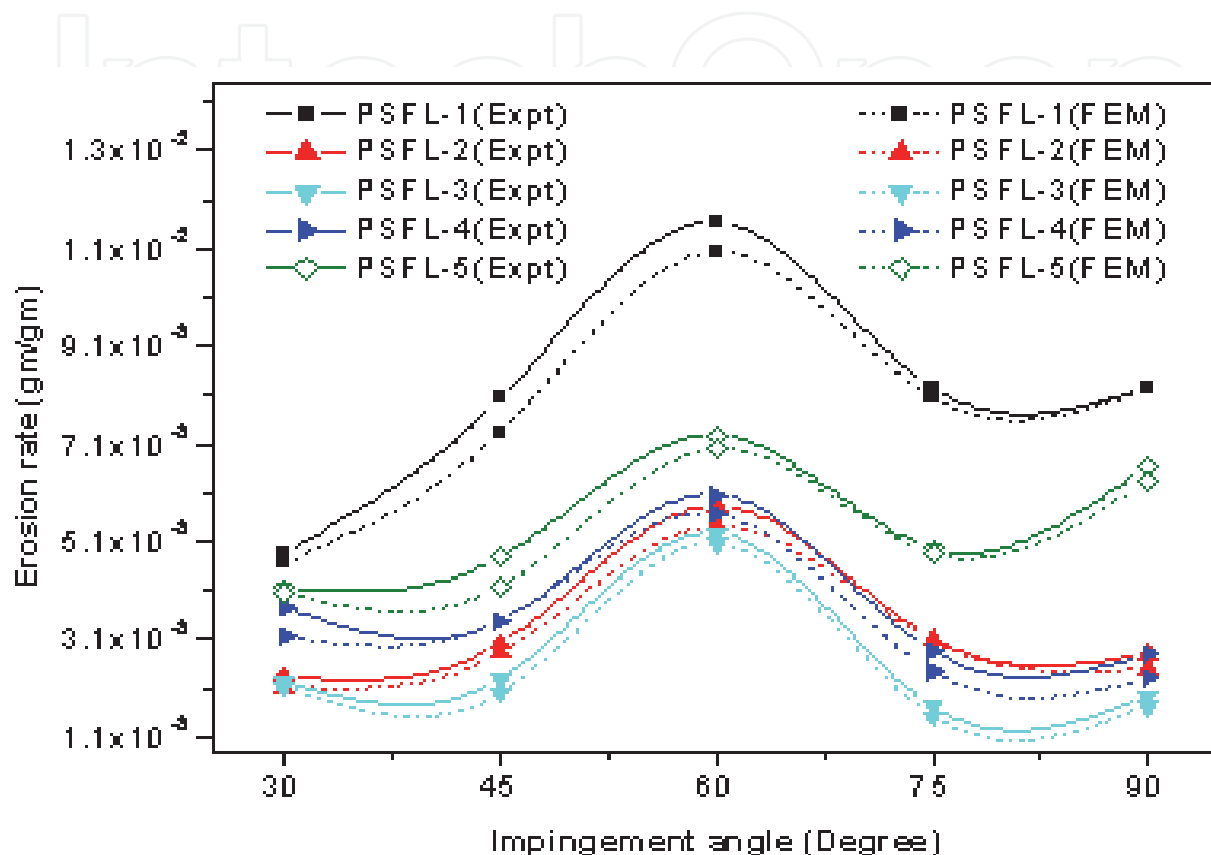


Fig. 3. Influence of impingement angle on erosion rates of unfilled glass fiber-polyester composites (Impact velocity: 43m/sec, stand-off distance: 75mm and erodent size: 450µm).

Micrograph (Figure 4c) of eroded surface of 20wt% glass fiber based composite shows deeper micro-cracks on the composite surface due to brittle nature of polyester resin. However, the normal impact did not result in higher erosion rate like brittle materials. During normal impact the largest part of the initial energy is converted into heat and hence matrix is softened which resulted in embedment of sand particles (Figure 4d). The embedded sand particles control the further erosion of the target surface. Figures 4e and 4f shows micrographs of eroded surfaces of 30wt% and 40 wt% glass fiber reinforced polyester composite respectively. At oblique impingement angle (60°), micrographs (Figures 4e and 4f) show matrix is plastically deformed and amount of deformation is proportional to impact velocity of particles. At 43 m/sec impact velocity removal of matrix along the length of the fiber and subsequently getting removed can be seen from the micrograph (Figure 4e). At same impact velocity for 40wt% glass fiber based composite little high degree of plastic deformation and removal of matrix and hence fibers protruded out from the matrix can be

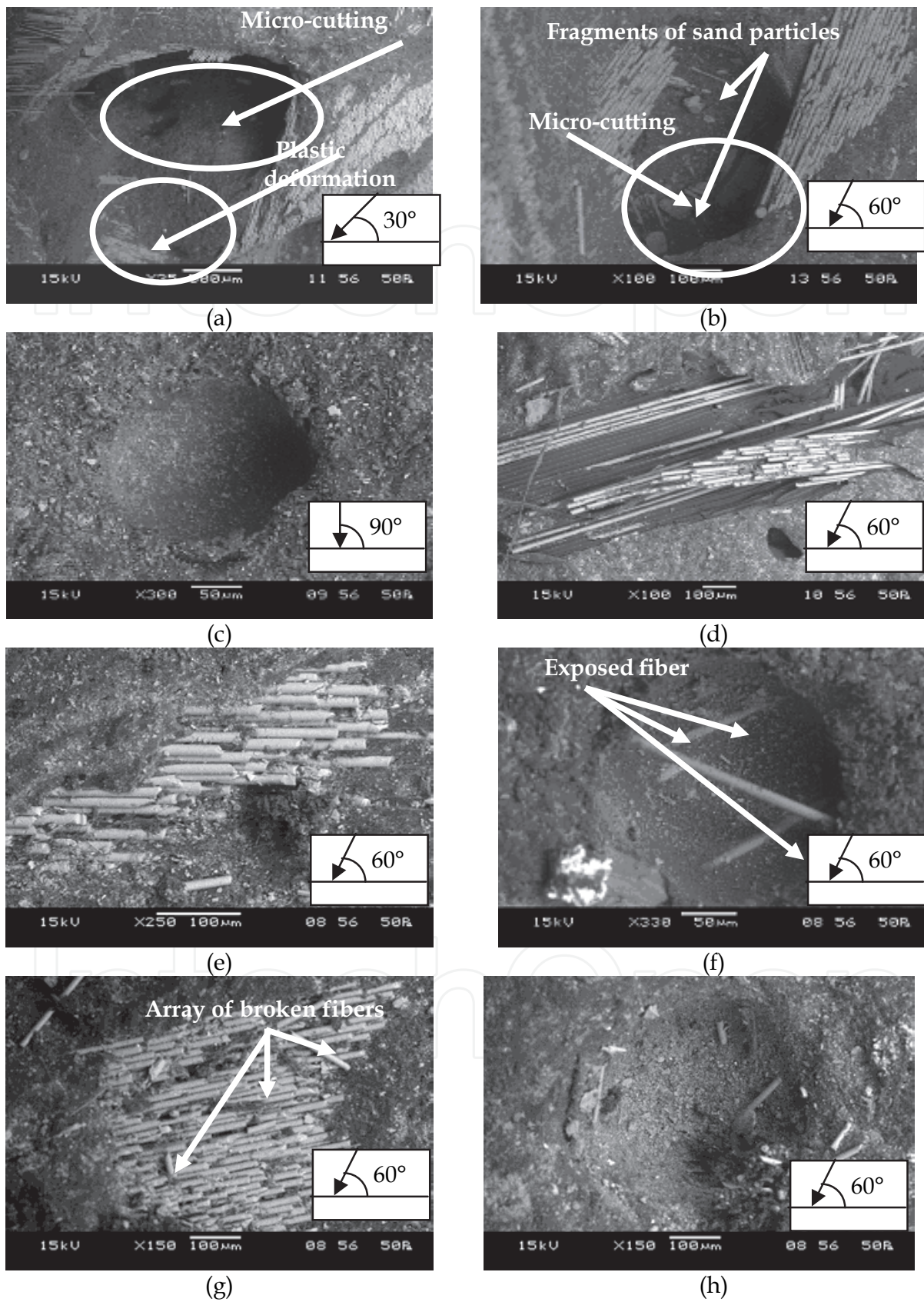


Fig. 4. SEM micrographs of the eroded surfaces of the unfilled glass fiber-polyester composites

seen in the micrograph (Figure 4f). Similarly, for 50wt% glass fiber based composites (Figures 4g, h) show similar behaviour as shown in Figures 4e and 4f but the target surface is completely eroded out and exposure of glass fibers at 60° impingement angle. The exposed fibers are broken into small fragments resulting in excessive wear.

3.1.3 Influence of impact velocity

In order to study the effect of impact velocity on erosion rate, erosion tests are performed on the short glass fiber reinforced polyester composites by varying the impact velocity from 43 to 65 m/s. As seen in Figure 5, erosive wear rates of the samples are remarkably higher with the increase in impact velocity conforming to the theoretical expectations. Particles have a higher kinetic energy at higher impact velocity, which results in greater impingement effect and results in increased erosion rate.

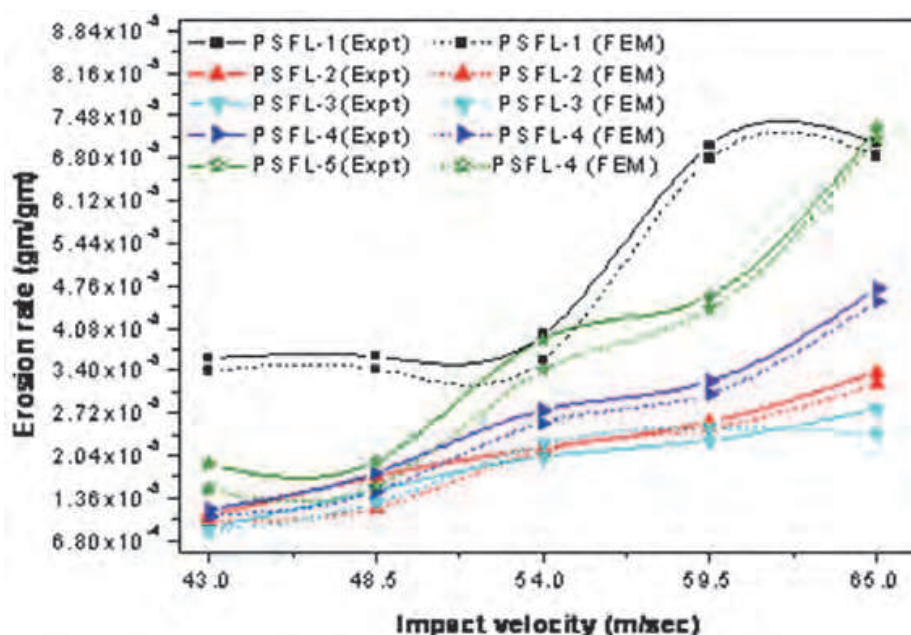


Fig. 5. Influence of impact velocity on erosion rates of unfilled glass fiber-polyester composites (Impingement angle: 60°, stand-off distance: 75mm and erodent size: 450µm).

It is clear from Figure 5 that steady-state erosion rate of all the composites increases with increase in impact velocity. Similarly, in computationally the finite element simulated results seems to be parallel to the experimental results as shown in Figure 5. It was observed that the composite with 30 wt% of short glass fiber reinforced composite is most resistant to erosion rate followed by the composites with 20, 50 and 40 wt% fiber contents in a decreasing order. Thus it is clearly from Figure that velocity of the erosive particles has a very strong significant effect on erosion rate however, their real mechanistic aspects may need further investigation.

3.2 Steady state erosion rate (for particulate filled composites)

3.2.1 Influence of impingement angle

In case of CBPD filled short glass fiber-polyester composites, the erosion rate increases monotonically with the increase in impingement angle and reaches maximum at 60°

impingement angle for both particulate filled composites and unfilled composite. However, particulate filled composites shows lesser erosion rate as compared to unfilled composites as shown in Figure 6.

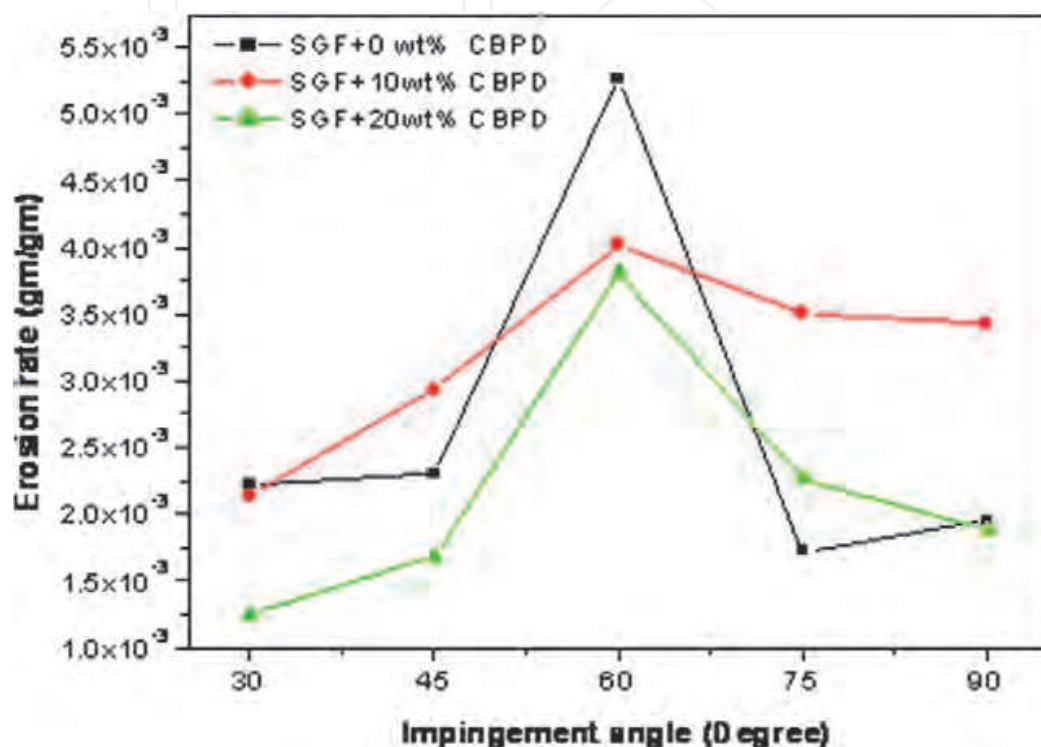


Fig. 6. Influence of impingement angle on erosion rates of particulate filled composites (Impact velocity: 43 m/sec, stand-off distance: 75mm and erodent size: 450 μ m).

At low impingement angle the surface damage is seemed to be less and the erosion rate is also very low. Earlier studies have also reported that the crack length decreases with decreasing angle, i.e. at lower impingement angle it is small and attain maximum towards 90° (Suresh & Harsa, 2006). Longer cracks imply more rapid erosion rate taking place and the volume of material removal is approximately proportional to square of the surface crack length. This has only happened in case of normal impact velocity and hence the erosion rate shows stronger dependence on impact velocity and the angle of impingement. The maximum erosion rate for unfilled and particulate filled composites show at an angle of 60° as shown in Figure 6 under similar condition as studied in case of unfilled composites (Figure 4). But earlier studies have proved that two different processes contribute erosion on brittle materials, i.e. when particles impact at near normal incidence, lateral cracks induce mass loss, but the radial cracks do not contribute significantly to materials removal. For impact at oblique incidence, however, radial cracks can lead to materials removal (John Rajesh et al., 2001). In the present study, all the composites neither show brittle response nor does it behave ductile. It shows semi-brittle-ductile nature as shown in Figure 6.

3.2.2 Influence of impact velocity

Similarly, the variation of erosion rate of unfilled and CBPD filled composites with impact velocity is shown in Figure 7. Erosion trials are conducted at five different impact velocities. It is seen, in this figure that for all the composite samples, the erosion rates gradually increases by the increase in impact velocity. The increase in erosion rate with impact velocity can be attributed to increased penetration of particles on impact as a result of dissipation of greater amount of particle thermal energy to the target surface. This leads to more surface damage, enhanced sub-critical crack growth etc. and consequently to the reduction in erosion resistance.

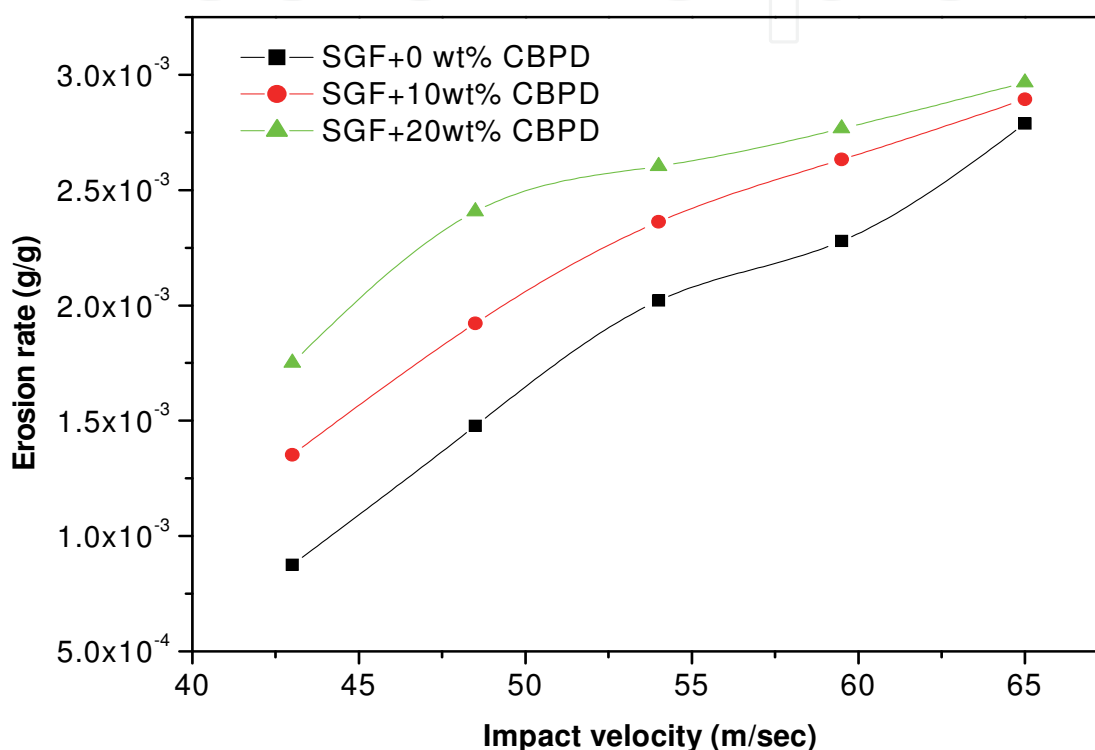


Fig. 7. Influence of impact velocity on erosion rates of particulate filled composites (Impingement angle: 60°, stand-off distance: 75mm and erodent size: 450µm).

3.2.3 Taguchi analysis and response optimization

As an evaluation tool for determining robustness, the signal-to-noise (S/N) ratio is the most important component of a parameter design. In the Taguchi method, the term 'signal' represents the desirable target i.e. erosion rate and the term 'noise' represents the undesirable value. The analysis is made using the computational software used for design of experiment applications (MINITAB 15). The response table (S/N ratio) for erosion rate is mentioned in Table 3. The overall mean for the S/N ratio of erosion rate is found to be 61.76db. Effect of control factors on erosion rate is shown in Figure 8. It is clear from Figure that factors A₁, B₃, C₁, D₃ and E₃ have been observed to be the most significant level which experimentally influences the erosion rate on the basis of smaller-the-better characteristics. The respective interaction plots are observed in the Figures 9a-c.

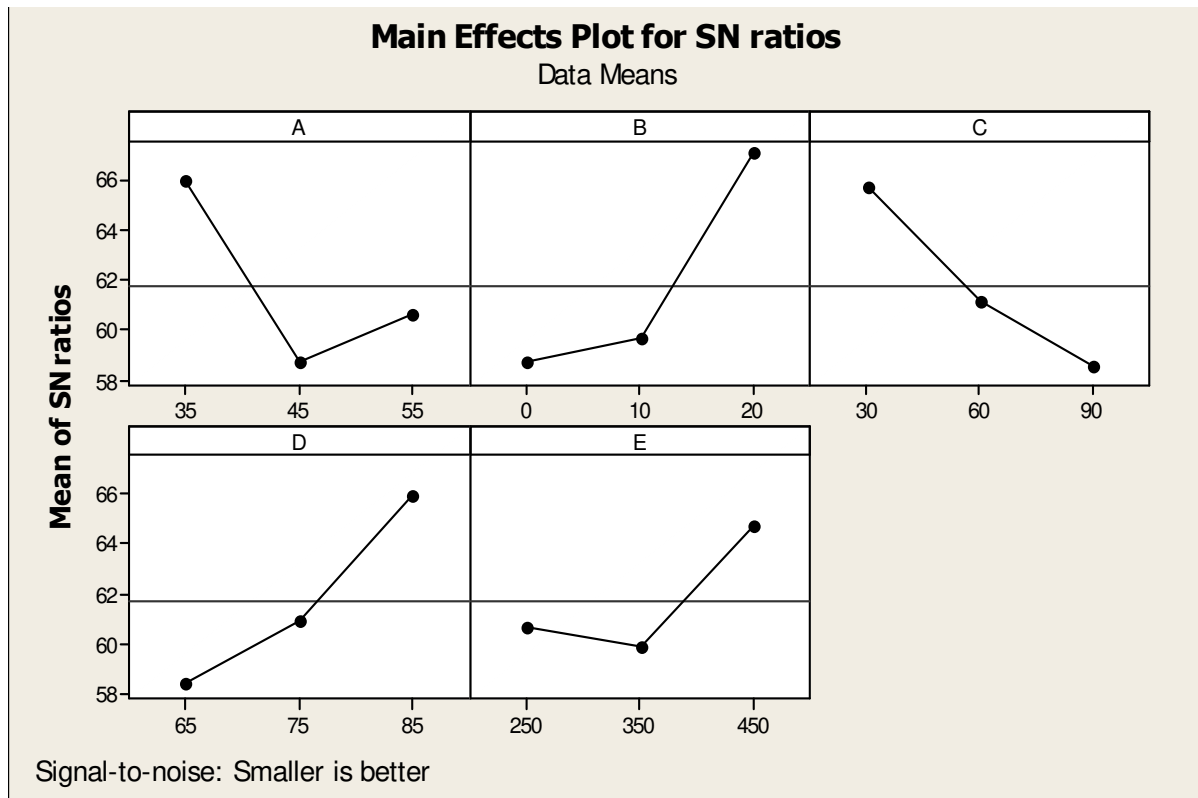


Fig. 8. Effect of control factors on erosion rate

3.2.4 Surface morphology of Taguchi experimental results

To verify the erosion mechanisms of glass fiber reinforced polyester composites, eroded surfaces of the composites are observed as per Taguchi experimental orthogonal array design (see Table 3) by scanning electron microscopy (SEM). Figure 10a, 10b shows the SEM micrographs of eroded composite sample studied at lower impingement angle (see Table 3, Experiment 1) shows the random distribution of short glass fiber and removable of matrix material on the composite surface. Figures 10c and 10d show for 10wt% of CBPD filler composite that the erosion rate decreases (see Table 3, Experiment 6) with lower particle size (250 μm). When the erodent particle size is more (450 μm) (see Table 3, Experiment 5), it has more energy to chip-off the target material as shown in Figure 10d. But in the case of a small particle size, it has insufficient energy to create the crack in the target material and thus lead to low erosion rate. In other hand, when the erodent particle strikes the composite surface, at 90° impingement angle the fiber damage resulting from recurring micro-ploughing in combination with the fibers getting slowly worn out from the matrix surfaces are observed. But it is not the case as tested same composite with 350 μm particle size with impingement angle 60° (Figure 10e, f) shows more erosive surface with higher erosion rate (see Table 3, Experiment 4).

It has been discussed that the impact on brittle materials at an oblique angle produced radial cracks at an angle to the surface and they can contribute to only matrix material loss (Scattergood et al., 1981; Lawn, 1993). Radial cracks can also contribute to material loss when they drive through a relatively thin wall. In such a case, the material loss will occur without the formation of a lateral crack. Larger erodents produce deeper radial cracks. The tendency

for material loss to occur from radial cracking should increase with erodent diameter (Lee et al., 2005; Milman et al., 1999). With the increasing of the CBPD particles in the composites from 10wt% to 20wt%, the wear rate of the composites increased gradually, reached a maximum and then declined gradually. The peak wear resistance for 20wt% CBPD particulate filled glass-polyester composites shows 60° impingement angle (see Figure 6). As shown from Figure 10f, the worn surface of particulate filled glass fiber-polyester composites when 350µm erodent particle strikes at an impact velocity 54m/sec the composite surface at lower impingement angle (30°) (see Table 3, Experiment 16) shows only removal of matrix material on the composite surface. Figure 10g shows a hole formed after

| Expt. No. | Impact Velocity (A)(m/s) | CBPD content (B) (%) | Impingement angle (C) (Degree) | Stand-off Distance (D)(mm) | Erodent size (E) (µm) | Erosion rate (Er) (gm/gm) | S/N Ratio (db) |
|-----------|--------------------------|----------------------|--------------------------------|----------------------------|-----------------------|---------------------------|----------------|
| 1 | 43 | 0 | 30 | 65 | 250 | 0.0003303 | 69.6224 |
| 2 | 43 | 0 | 60 | 75 | 350 | 0.0002466 | 72.1588 |
| 3 | 43 | 0 | 90 | 85 | 450 | 0.0001246 | 78.0908 |
| 4 | 43 | 10 | 30 | 75 | 350 | 0.0008917 | 60.9959 |
| 5 | 43 | 10 | 60 | 85 | 450 | 0.0005550 | 65.1141 |
| 6 | 43 | 10 | 90 | 65 | 250 | 0.0047442 | 46.4768 |
| 7 | 43 | 20 | 30 | 85 | 450 | 0.0001267 | 77.9468 |
| 8 | 43 | 20 | 60 | 65 | 250 | 0.0005667 | 64.9334 |
| 9 | 43 | 20 | 90 | 75 | 350 | 0.0012350 | 58.1667 |
| 10 | 54 | 0 | 30 | 75 | 450 | 0.0014625 | 56.6981 |
| 11 | 54 | 0 | 60 | 85 | 250 | 0.0028121 | 51.0194 |
| 12 | 54 | 0 | 90 | 65 | 350 | 0.0027000 | 51.3727 |
| 13 | 54 | 10 | 30 | 85 | 250 | 0.0001375 | 77.2339 |
| 14 | 54 | 10 | 60 | 65 | 350 | 0.0033938 | 49.3864 |
| 15 | 54 | 10 | 90 | 75 | 450 | 0.0041087 | 47.7258 |
| 16 | 54 | 20 | 30 | 65 | 350 | 0.0008175 | 61.7502 |
| 17 | 54 | 20 | 60 | 75 | 450 | 0.0001844 | 74.6860 |
| 18 | 54 | 20 | 90 | 85 | 250 | 0.0011706 | 58.6316 |
| 19 | 65 | 0 | 30 | 85 | 350 | 0.0024783 | 52.1171 |
| 20 | 65 | 0 | 60 | 65 | 450 | 0.0045143 | 46.9082 |
| 21 | 65 | 0 | 90 | 75 | 250 | 0.0031857 | 49.9359 |
| 22 | 65 | 10 | 30 | 65 | 450 | 0.0005443 | 65.2835 |
| 23 | 65 | 10 | 60 | 75 | 250 | 0.0012014 | 58.4060 |
| 24 | 65 | 10 | 90 | 85 | 350 | 0.0005114 | 65.8243 |
| 25 | 65 | 20 | 30 | 75 | 250 | 0.0003300 | 69.6297 |
| 26 | 65 | 20 | 60 | 85 | 350 | 0.0004295 | 67.3403 |
| 27 | 65 | 20 | 90 | 65 | 450 | 0.0003138 | 70.0667 |

Table 3. Experimental design using L₂₇ orthogonal array

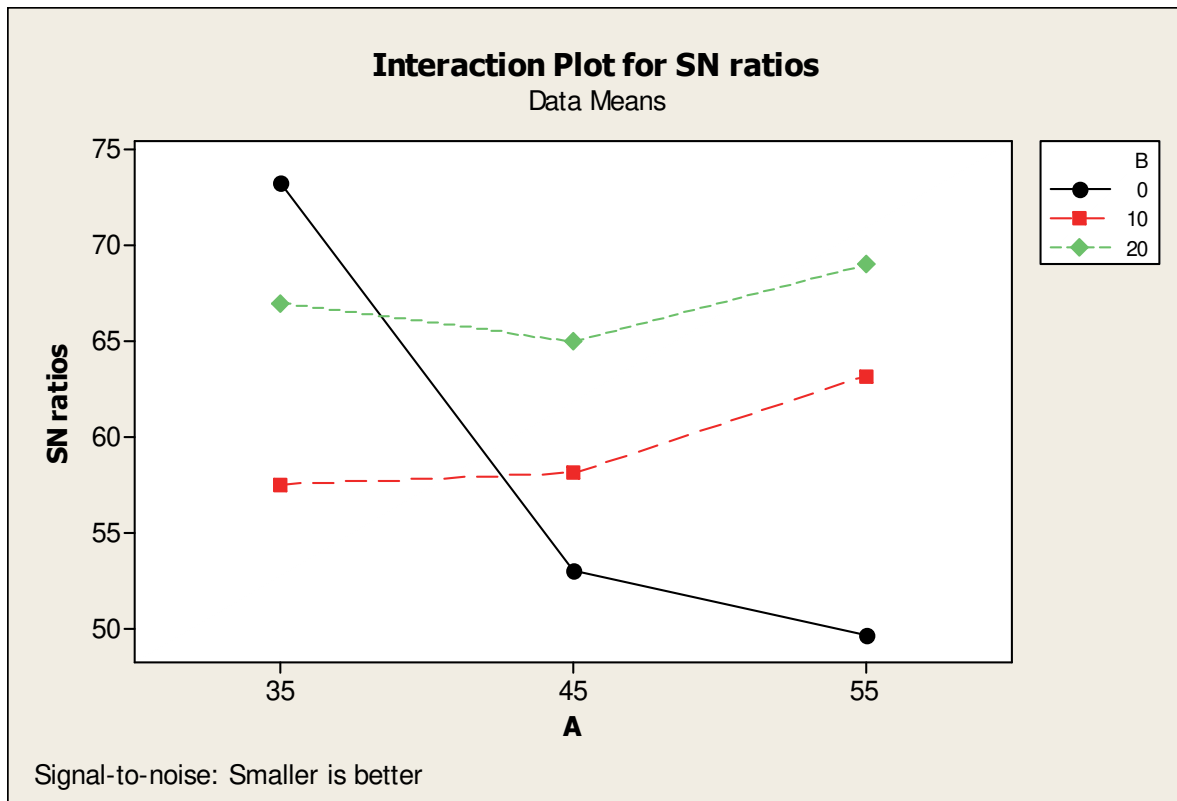


Fig. 9a. Interaction graph between factor A and factor B ($A \times B$) for erosion rate

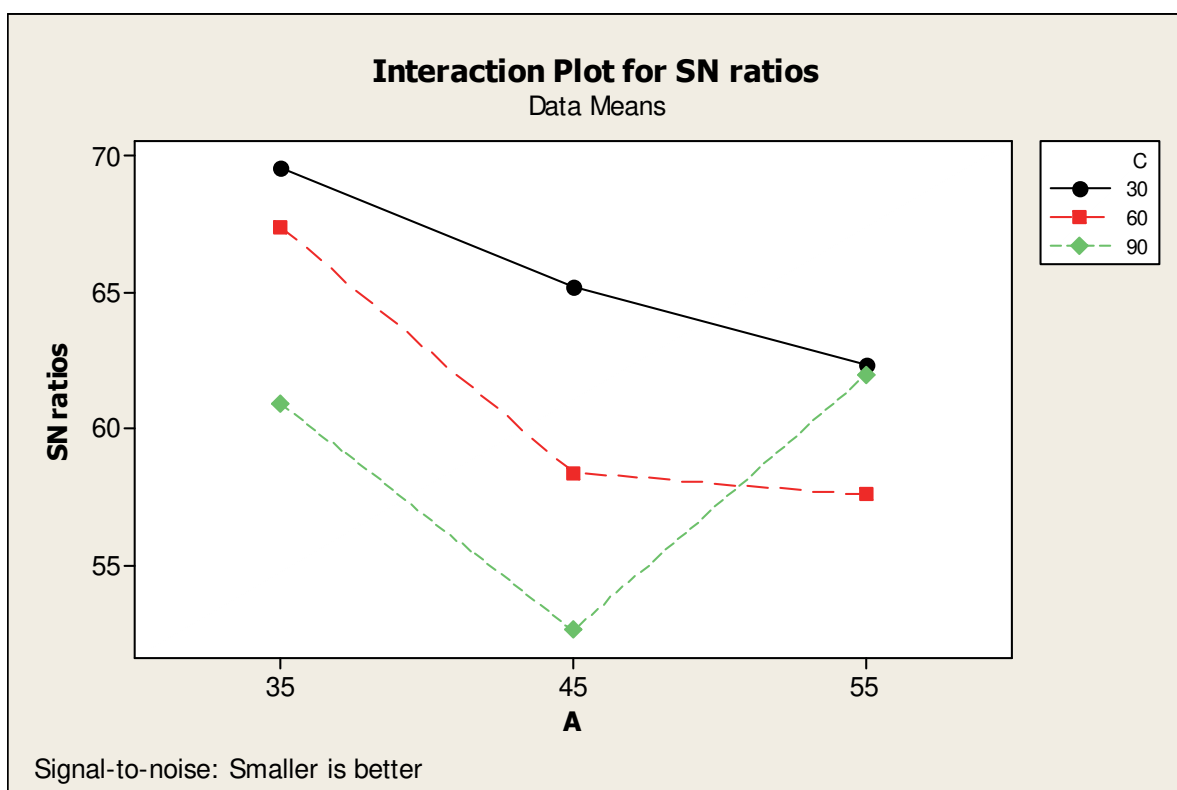


Fig. 9b. Interaction graph between factor A and factor C ($A \times C$) for erosion rate

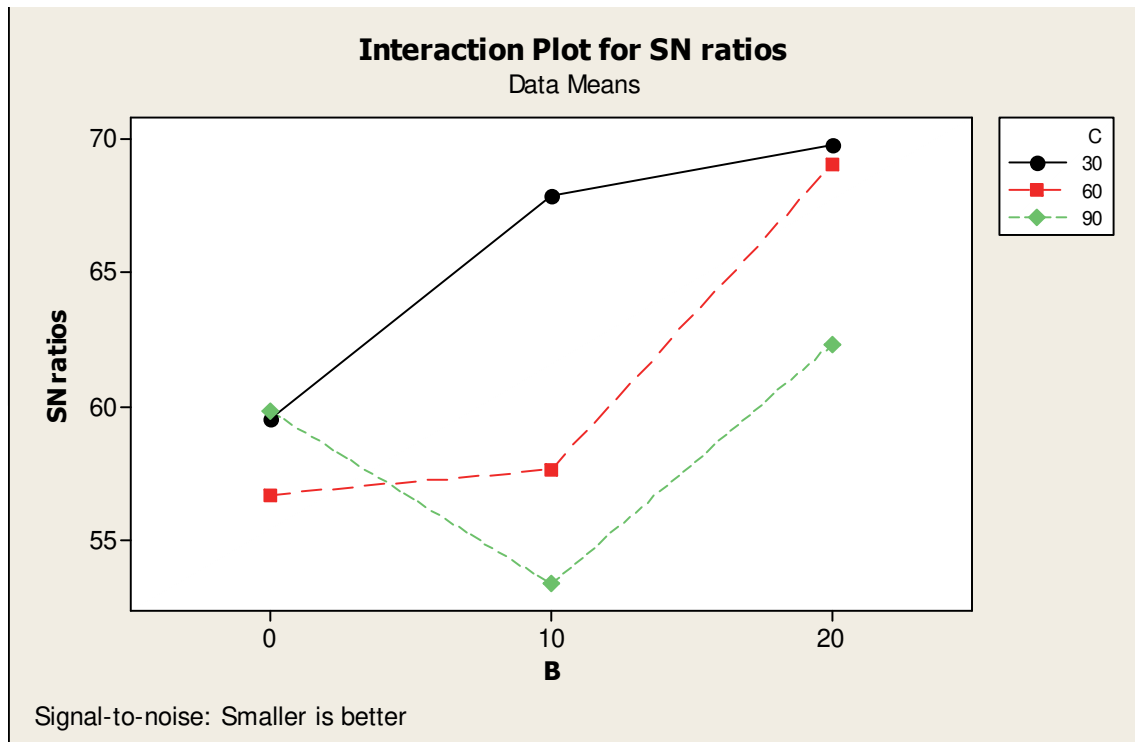
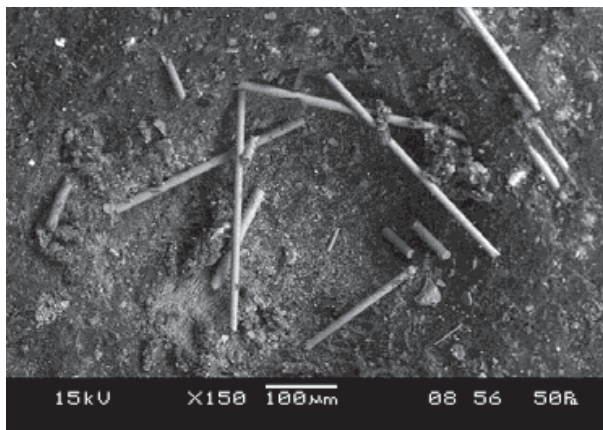
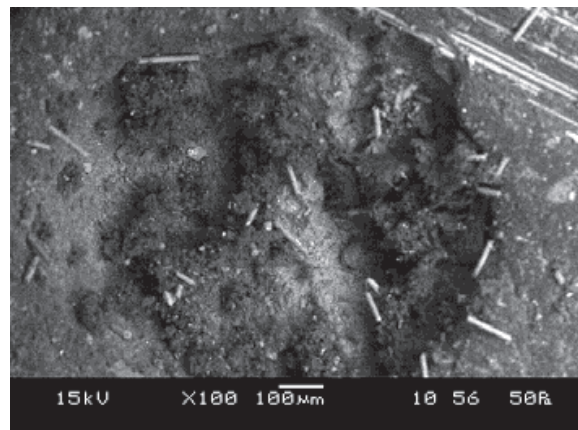


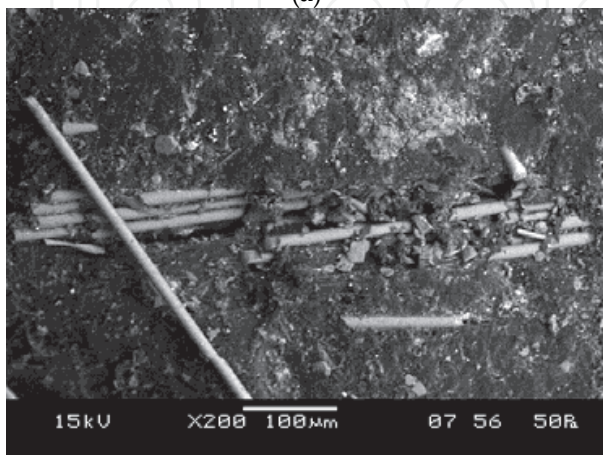
Fig. 9c. Interaction graph between factor B and factor C (B×C) for erosion rate



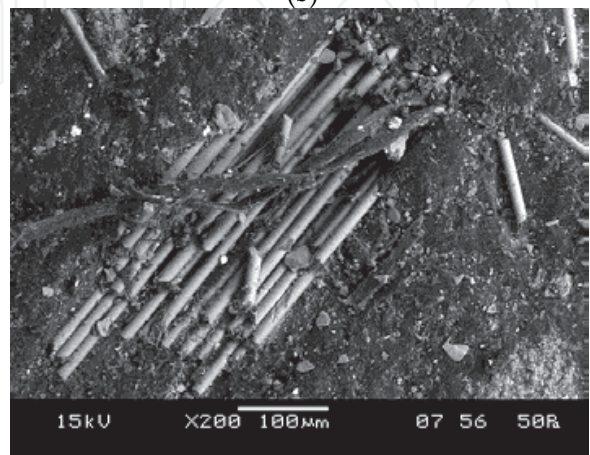
(a)



(b)



(c)



(d)

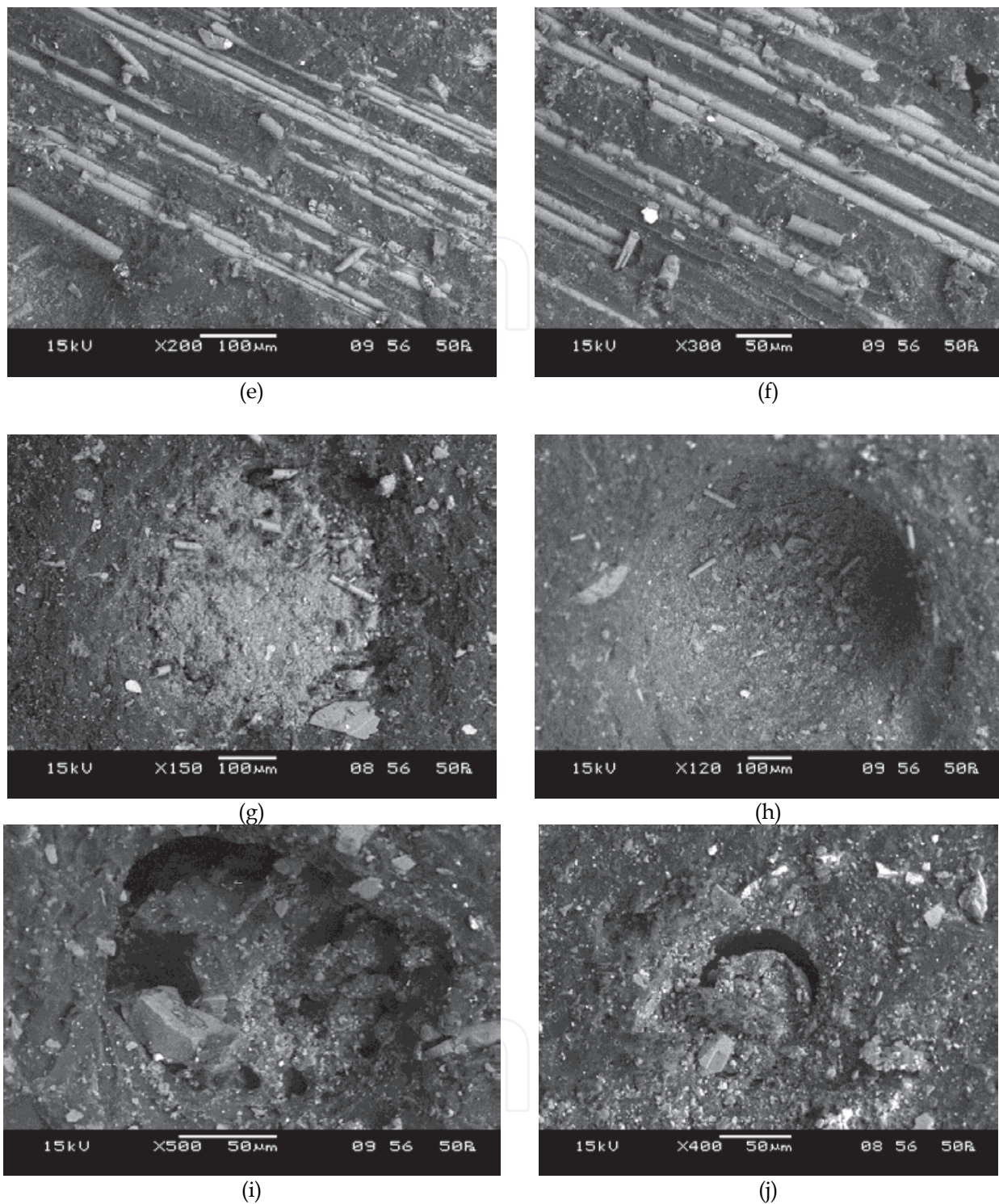


Fig. 10. SEM micrographs of the eroded glass fiber-polyester composites filled with CBPD

an CBPD particle is removed from the surface. The inside surface of the hole seemed very smooth and clear which indicated that one CBPD particle wholly debonded from the matrix with the propagation of interfacial cracks (Figure 10h) due in part to the poor interfacial bond strength. However, on further increase in erodent particle from 250μm to 350μm size and impingement angle from 30° to 60° (see Table 3, Experiment 26) the matrix materials

removed from the surface along with exposure of glass fibers as shown in Figure 10i. The excessive amount of material loss in the composite is due to, too much CBPD particles were added (20 wt%), the interface area may have been too large and particles may have touched directly, so interfacial defects and cracks could largely emerge. Thus, CBPD particles could be more easily removed and could not improve the wear resistances. So the wear resistance of the composites declined with the increased content of the CBPD particles. In Figure 10j, an CBPD particle with a flat top surface protruding slightly over the worn surface, around whose back half interface distributed a clear gap (see Table 3, Experiment 25). The morphology showed that the top surface of the CBPD particle was heavily polished and became flat by the impact of the erodent particles with high velocity (65m/sec) at an angle of 60°, and the back part of the CBPD particle debonded and slipped from the matrix along the interface.

3.3 ANOVA and the effects of factors

Table 4 shows the results of the ANOVA with the erosion rate (E_r) for CBPD filled short glass fiber reinforced polyester composites. The objective of ANOVA is to analyze the influence of impact velocity (A), CBPD content (B), impingement angle (C), stand-off distance (D) and erodent size (E) on the total variance of the results. This analysis was undertaken for a level of significance of 5% that is for a level of confidence of 95%.

| Source | DF | Seq SS | Adj SS | Adj MS | F | P |
|--------|----|---------|--------|--------|------|-------|
| A | 2 | 252.51 | 252.51 | 126.26 | 2.53 | 0.195 |
| B | 2 | 377.09 | 377.09 | 188.54 | 3.77 | 0.120 |
| C | 2 | 240.40 | 240.40 | 120.20 | 2.41 | 0.206 |
| D | 2 | 262.48 | 262.48 | 131.24 | 2.63 | 0.187 |
| E | 2 | 121.18 | 121.18 | 60.59 | 1.21 | 0.388 |
| A×B | 4 | 809.70 | 809.70 | 202.42 | 4.05 | 0.102 |
| A×C | 4 | 163.40 | 163.40 | 40.85 | 0.82 | 0.575 |
| B×C | 4 | 211.27 | 211.27 | 52.82 | 1.06 | 0.479 |
| Error | 4 | 199.89 | 199.89 | 49.97 | | |
| Total | 26 | 2637.93 | | | | |

Table 4. ANOVA table for erosion rate

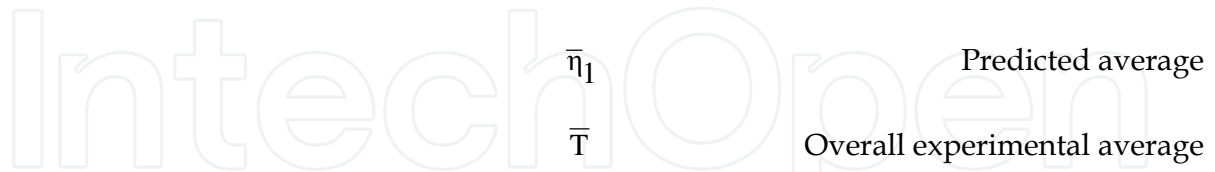
From Table 4 it is observed that CBPD content ($p = 0.120$), stand-off distance ($p = 0.187$), impact velocity ($p = 0.195$) and impingement angle ($p = 0.206$) have great influence on the out put performance (erosion rate). The interactions of impact velocity and CBPD content ($p = 0.102$) has greater significant influence on erosion rate but the factor erodent size ($p = 0.388$), interaction between impact velocity and impingement angle ($p = 0.575$) and CBPD content and impingement angle ($p = 0.479$) have less significant contribution on erosion rate.

3.4 Confirmation experiment

The confirmation experiment is the final step in the first iteration of the design of experiment process. The purpose of the confirmation experiment is to validate the conclusions drawn during the Taguchi experimental design process. The confirmation experiment is performed by conducting a new test condition in combination of the significant factors and their

interaction levels on erosion rate as reported in Table 4. The final step is to predict and verify the improvement of the erosion resistance. The predictive value $\bar{\eta}_1$ using the optimal levels of the input parameters can be calculated as:

$$\bar{\eta}_1 = \bar{T} + (\bar{A}_2 - \bar{T}) + (\bar{B}_2 - \bar{T}) + [(\bar{A}_2\bar{B}_2 - \bar{T}) - (\bar{A}_2 - \bar{T}) - (\bar{B}_2 - \bar{T})] + (\bar{C}_3 - \bar{T}) + (\bar{D}_2 - \bar{T}) \quad (3)$$



$\bar{A}_2, \bar{B}_2, \bar{C}_3$ and \bar{D}_2 Mean response for factors and interactions at designated levels.

By combining like terms, the equation reduces to

$$\bar{\eta}_1 = \bar{A}_2\bar{B}_2 + \bar{C}_3 + \bar{D}_2 - 2\bar{T} \quad (4)$$

After solving the above predictive equation the erosion rate is found to be $\bar{\eta}_1 = 51.03$ dB and the experimental result is 51.54 dB. The resulting model seems to be capable of predicting wear rate to a reasonable level of accuracy. An error of 1.78% for the S/N ratio of wear rate is observed. This validates the development of the mathematical model for predicting the measures of performance based on knowledge of the input parameters.

4. Conclusions

1. The particle reinforced composites show good tribological properties. The erosion rate for unfilled composites 30wt% glass fiber polyester composites show better erosion resistance whereas, for particulate filled composites 20wt% filled content shows superior erosion resistance as compared with the rest of the filled and unfilled composites.
2. The variation of erosion rate with impingement angles, the material loss is dictated mainly more at 60° impingement angles, in the steady state erosion rate with other control factors are remain constant. However, compared with the experimental results, the FE model (ANSYS/AUTO-DYN) is much closer to the experimental results. The major advantages of simulated results are during experimental study it is very difficult to analysis the flow direction and particularly at low impingement angle most of the erodent particles are sliding on the target material instead of reback of erodent particles. However, in finite element simulated model the above conditions can be measured easily including the residual stress and the depth of penetration which is difficult to determine by experimental method.
3. In eroded samples observed in scanning electron microscope shows mostly two types of wear mechanisms i.e. micro-cutting and micro-ploughing actions. It shows formation of lips and their flow along the direction of the erodent. At a medium angle of impingement (60°), the material loss is governs mostly by cutting action. It also depicts formation of coarser and larger lips. At a higher angle of impingement (90°), the material loss is dictated by micro-fracturing mechanism. However, CBPD particulates provide the protection against erosive wear in the composite.

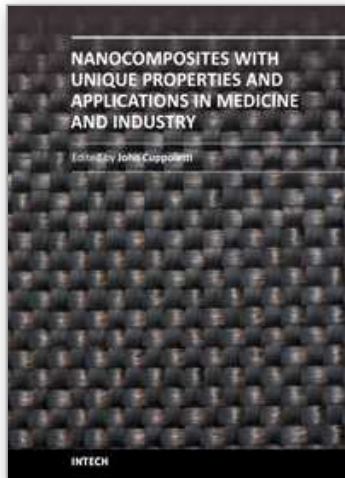
5. Acknowledgement

The authors are grateful to the financial supports of the research project Ref. No. SR/FTP/ETA-49/08 by Department of Science and Technology, India.

6. References

- Adler, W.F. (1995). Waterdrop Impact Modeling, *Wear*, Vol. 186-187, pp. 341-351.
- Al-Jabri, K. S.; Taha, R. A.; Al-Hashmi, A. & Al-Harthy A. S. (2006). Effect of Copper Slag and Cement By-pass Dust addition on Mechanical Properties of Concrete, *Construction and Building Materials*. Vol. 20, pp. 322-331.
- Batis, G.; Rakanta, E.; Sideri, E.; Chaniotakis, E. & Papageorgiou, A. (2002). Advantages of Simultaneous use of Cement Kiln Dust and Blast Furnace Slag, *In: Proceedings of the International Conference on Challenges of Concrete Construction*, University of Dundee, Dundee, UK.
- Biswas, S. & Satapathy, A. (2009). Tribo-Performance Analysis of Red Mud Filled Glass-Epoxy Composites Using Taguchi Experimental Design, *Materials & Design*, Vo. 30, No. 8, pp. 2841-2853.
- Biswas, S. & Satapathy, A. (2010). A Comparative Study on Erosion Characteristics of Red Mud Filled Bamboo-Epoxy and Glass-Epoxy Composites, *Materials & Design*, Vol. 31, No. 4, pp.1752-1767.
- El-Sayed, H. A.; Gabr, N. A.; Hanafi, S. & Mohran, M. A. (1991). Re-utilization of By-pass Kiln Dust in Cement Manufacture, *In: Proceedings of the International Conference on Blended Cement in Construction*, Sheffield, UK.
- ElTobgy, M. S.; Ng, E. & Elbestawi, M. A. (2005). Finite Element Modeling of Erosive Wear, *International Journal of Machine Tools and Manufacture*, Vol. 45, pp. 1337-1346.
- Glen, S.P. (1993). *Taguchi Methods: A Hands-on Approach*, Addison-Wesley, New York.
- Hsu, S. M.; Shen, M. C. & Ruff, A. W. (1997). Wear Prediction for Metals, *Tribology International*, Vol. 30, No. 5, pp. 377-383.
- Hutchings, I. M. (1992). Ductile brittle transitions and wear maps for the erosion and abrasion of brittle materials, *Journal of Physics D: Applied Physics*, Vol. 25, pp. A212-A221.
- John Rajesh, J.; Bijwe, J.; Tewari, U. S. & Venkataraman, B. (2001). Erosive Wear Behaviour of Various Polyamides, *Wear*, Vol. 249, pp. 702-714.
- Komvopoulos, K. & Choi, D. H. (1992). Elastic Finite Element Analysis of Multi-Asperity Contacts, *ASME Journal of Tribology*, Vol.114, pp. 823-831.
- Krazowski, L. & Emery, J J. (1981). Use of Cement Kiln Dust as a filler in Asphalt Mixes, *In: Proceedings, ORF/CANMET Symposium on Mineral Fillers*, Ontario Research Foundation, Toronto.
- Lawn, B. (1993). *Fracture in Brittle Solids*, 2nd ed., Cambridge University Press, Cambridge, UK.
- Lee, S. H., Lee, Y. I.; Kim, Y.W.; Xie, R. J.; Mitomo, M. & Zhan, G. D. (2005). Mechanical Properties of Hot-Forged Silicon Carbide Ceramics, *Scripta Materialia*, Vol. 52, pp. 153-156.
- Ling, F. F. & Pan C. H. T. (1986). Approaches to Modeling of Friction and Wear, *Proceedings of the Workshop on the Use of Surface Deformation Models to Predict Tribology Behavior*, Springer-Verlag, New York.

- Ludema, K. C. & Bayer, R. G. (1991). Tribological Modeling for Mechanical Designers, ASTM STP1105, *American Society for Testing and Materials*, Philadelphia.
- Milman, Y.V.; Chugunova, S. I.; Goncharova, I. V.; Chudoba, T.; Lojkowski, W. & Gooch, W. (1999). Temperature Dependence of Hardness in Silicon-Carbide Ceramics with Different Porosity, *International Journal of Refractory Metals and Hard Materials*, Vol. 17, No. 5, pp. 361-368.
- Patnaik, A.; Kaundal, R.; Satapathy, A.; Biswas, S. & Pradeep K. (2010a). Solid Particle Erosion of Particulate Filled Short Glass Fiber Reinforced Polyester Resin Composites, *Advanced Materials Research*, Vol.123-125, pp. 213-216.
- Patnaik, A.; Abdulla, Md., Satapathy, A.; Biswas, S. & Satapathy, B. K. (2010b). A Study on Possible Correlation between Thermal Conductivity and Wear Resistance of Particulate Filled Polymer Composites, *Materials and Design*, Vol. 31, pp. 837-849.
- Patnaik, A.; Satapathy, A.; Chand, N.; Barkoula, N. M. & Biswas, S. (2010c). Solid Particle Erosion Wear Characteristics of Fiber and Particulate Filled Polymer Composites: A Review, *Wear*, Vol. 68, No. (1-2), pp. 249-263.
- Patnaik, A.; Satapathy, A.; Dwivedy, M. & Biswas, S. (2010d). Wear behaviour of Plant-fiber (Pine-Bark) and Cement-kiln-dust Reinforced Polyester Composites using Taguchi Experimental Model, *Journal of Composite Materials*, Vol. 44, No. 5, pp. 559-574.
- Patnaik, A.; Tejyan, S. & Rawal, A. (2010e). Solid Particle Erosion Behavior of Needle-punched Nonwoven Reinforced Composites, *Research Journal of Textile and Apparel*, Vol. 14, No. 3, pp. 12-22.
- Patnaik, A.; Satapathy, A., Mahapatra, S. S. & Dash. R. R. (2010f). Modified Erosion Wear Characteristics of Glass-Polyester Composites by Silicon Carbide Filling: A Parametric Study using Taguchi Technique, *International Journal of Materials and Product Technology (Materials Processing Technology)*, Vol. 38, No. 2-3, pp.131-152.
- Patnaik, A.; Mahapatra, S. S. & Dash, R. R. (2010g). Flyash Filling for Improved Wear Resistance of Glass-Polyester Composites : An Experimental Study, *The Journal of Solid Waste Technology and Management*, Vol. 36, No. 1, pp.26-37.
- Rothon, R. N. (2002). Particulate Fillers for Polymers, *RAPRA Review Reports*, Vol. 12, No. 9, pp. 164.
- Routbort, J. L.; Gulden, M. E. & Marshall, E. (1981). Particle Size Distribution Effects on the Solid Particle Erosion of Brittle Materials, *Wear*, Vol. 71, pp. 363-373.
- Scattergood, R. O.; Routbort, J. L. & Turner, A. P. L. (1981). Velocity and Size Dependence of the Erosion Rates in Silicon, *Wear*, Vol. 67, pp. 227-232.
- Sri Ravindrarajah, R. (1982). Usage of Cement Kiln Dust in Concrete, *International Journal of Cement Composites and Lightweight Concrete*, Vol. 4, No. 2, pp. 95-102.
- Strzepa, P.; Zamirowski, E. J.; Kupperman, J. B.; Goretta, K. C. & Routbort, J. L. (1993). Indentation, Erosion and Strength Degradation of Silicon-Alloyed Pyrolytic Carbon, *Journal of Materials Science*, Vol. 28, pp. 5917-5921.
- Suresh, A. & Harsha, A. P. (2006), Study of Erosion Efficiency of Polymers and Polymer Composites, *Polymer Testing*, Vol. 25, pp. 188-196.
- Tsuda, K.; Kubouchi, M.; Sakai, T.; Saputra, A. H. & Mitomo, N. (2006) General Method for Predicting the Sand Erosion Rate of GFRP, *Wear*, Vol. 260, pp. 1045-1052.
- Woytowicz, P. J. & Richman, R. H. (1999). Modeling of Damage from Multiple Impacts by Spherical Particles, *Wear*, Vol. 233-235, pp. 120-133.



Nanocomposites with Unique Properties and Applications in Medicine and Industry

Edited by Dr. John Cuppoletti

ISBN 978-953-307-351-4

Hard cover, 360 pages

Publisher InTech

Published online 23, August, 2011

Published in print edition August, 2011

This book contains chapters on nanocomposites for engineering hard materials for high performance aircraft, rocket and automobile use, using laser pulses to form metal coatings on glass and quartz, and also tungsten carbide-cobalt nanoparticles using high voltage discharges. A major section of this book is largely devoted to chapters outlining and applying analytic methods needed for studies of nanocomposites. As such, this book will serve as good resource for such analytic methods.

How to reference

In order to correctly reference this scholarly work, feel free to copy and paste the following:

Amar Patnaik, Sandhyarani Biswas, Ritesh Kaundal and Alok Satapathy (2011). Damage Assessment of Short Glass Fiber Reinforced Polyester Composites: A Comparative Study, Nanocomposites with Unique Properties and Applications in Medicine and Industry, Dr. John Cuppoletti (Ed.), ISBN: 978-953-307-351-4, InTech, Available from: <http://www.intechopen.com/books/nanocomposites-with-unique-properties-and-applications-in-medicine-and-industry/damage-assessment-of-short-glass-fiber-reinforced-polyester-composites-a-comparative-study>

INTECH

open science | open minds

InTech Europe

University Campus STeP Ri
Slavka Krautzeka 83/A
51000 Rijeka, Croatia
Phone: +385 (51) 770 447
Fax: +385 (51) 686 166
www.intechopen.com

InTech China

Unit 405, Office Block, Hotel Equatorial Shanghai
No.65, Yan An Road (West), Shanghai, 200040, China
中国上海市延安西路65号上海国际贵都大饭店办公楼405单元
Phone: +86-21-62489820
Fax: +86-21-62489821

© 2011 The Author(s). Licensee IntechOpen. This chapter is distributed under the terms of the [Creative Commons Attribution-NonCommercial-ShareAlike-3.0 License](#), which permits use, distribution and reproduction for non-commercial purposes, provided the original is properly cited and derivative works building on this content are distributed under the same license.

IntechOpen

IntechOpen